Key Engineering Materials
ISSN: 1662-9795, Vol. 926, pp 1969-1976
doi:10.4028/p-igbjg4

Submitted: 2021-12-07
Revised: 2022-02-24
Accepted: 2022-02-24
Online: 2022-07-22

Establishment of Thermal Deformation Constitutive Equation of TA15 Titanium Alloy

Shuo Guo[1,a], Gang Yang[1,2,b], Yuewen Zhai[1,c*], Leyu Zhou[1,d], Guojian Hao[1,e], Dehua Qiu[1,f]

[1*]Beijing Research Institute of Mechanical and Electrical Technology, Beijing 100083, China

[2]State Key Laboratory for Advanced Metals and Materials, University of Science and Technology Beijing, Beijing 100083, China

a,b authors are co-first authors of the article and contributed equally to this work

First authors: [a]rayshuo@iCloud.com, [b]mryangg@foxmail.com,

Corresponding author: [c]zhaiyuewen@163.com, [d]zhouleyu@ustb.edu.cn, [e]drhaogj@foxmail.com, [f]qiudh111@163.com

Keywords: TA15 titanium alloy, Flow stress, Constitutive equation.

Abstract: The hot deformation of TA15 titanium alloy was studied by the hot compression test on the Gleeble-3800 thermal simulation equipment. The true stress-strain curves of TA15 titanium alloy in the temperature range of 1123-1223K and the strain rate range of 0.001-1s^{-1} were obtained. The results show that the flow stress increases with decreasing temperature, and increases as the strain rate increases. And the deformation process is accompanied by work hardening and dynamic recovery and dynamic recrystallization. Based on the true stress-strain curves of TA15 titanium alloy, the Arrhenius-typed constitutive equation was established. The thermal deformation activation energy of TA15 titanium alloy with a strain of 0.2 is 746.27kJ/mol.

Introduction

TA15 titanium alloy has the advantages of high specific strength, low density, high corrosion resistance and good welding performance[1-4], and is widely used in aerospace, marine engineering and other fields, such as the complex force hermetically sealed cabin, beam frame and other key components[5-8].TA15 titanium alloy is a near-alpha titanium alloy with a nominal composition of Ti-6Al-2Zr-1Mo-1V. It is found that TA15 titanium alloy is very sensitive to temperature and strain rate during the forming process[9-1].

The microstructural evolution and deformation of TA15 titanium alloy have been studied by scholars.Li et al. established a unified mechanism material model of TA15 titanium alloy based on the softening mechanism of recrystallization and damage, and determined the optimal forming temperature range of 1023K~ 1173K for TA15 hot stamping[9]. Zhang et al. found that the peak stress σ_p, steady-state stress σ_{res},, peak strain ε_p and steady-state strain ε_{res} have linear relationships with the Zenner - Hollomon parameter, Z[10]. Li et al. studied the effect of deformation temperature and strain rate on flow stress and established a TA15 processing map[11].

The flow stress of titanium alloys is often predicted by using the the Arrhenius type of equations[12-16]. In this paper, the true stress-strain curve of TA15 titanium alloy in the temperature range of 1123-1223K and the strain rate range of 0.001-1s^{-1} were obtained by hot compression tests, and the constitutive equation was established based on the curve, and the thermal deformation microstruture of TA15 titanium alloy was analyzed to provide guidance for the hot working process of TA15 titanium alloy[17-23].

In this paper, the thermal deformation of TA15 titanium alloy was represented by setting different temperatures and strain rates. The temperature of hot compression tests was controlled below the phase change point . Flow stresses were further analyzed on the basis of the test results. A comprehensive model of temperature, strain rate and flow stresses was developed. Finally, the model was verified for reliability[24-26].

Procedure

The experimental material is cast TA15 titanium alloy, the chemical composition of the alloy is shown in Table 1, the main elements are Ti, Al, V, Zr, Mo, Fe. The original microstructure of the alloy is shown in Figure 1, which is a typical near-alpha microstructure consisting of α and β phases, and the crystal grain consists of lamellar (α+β) phases.

Table 1 Composition of TA15 titanium alloy (*wt*/%)

Al	V	Fe	Si	Zr	Mo	C	N	O	Ti
5.5-6.8	0.8-2.5	⩽0.3	⩽0.15	1.5-2.5	0.5-2.0	⩽0.13	⩽0.05	⩽0.16	Bal.

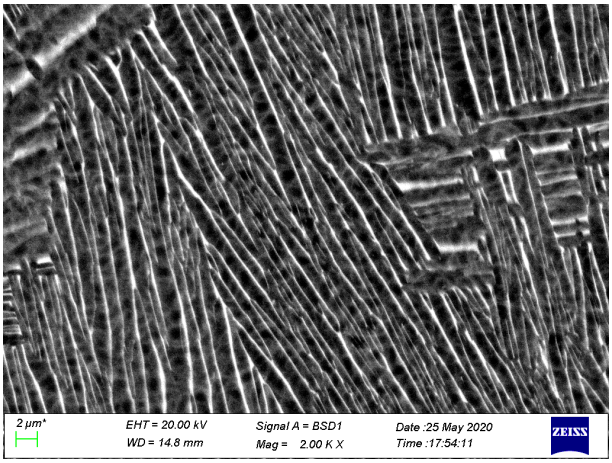

Figure 1 Microstructure of TA15 titanium alloy billet

Isothermal compression simulation tests are used to study the deformation and microsturcture evolution of materials at high temperatures. Isothermal compression tests of TA15 titanium alloy were performed on a Gleeble-3800 thermal simulator, and the height of the samples was reduced by 60% in the deformation temperature range of 1123-1223K and the strain rate range of 0.001-1s^{-1}. Cylindrical specimen of TA15 titanium alloy with a diameter of 8 mm and a height of 12 mm were fabricated. The appearance of the specimen before and after deformation is shown in the Figure 2a. Before hot compression, the samples would be heated and held for 5 min at a heating rate of 5 K/s, and then the experiments will be carried out at the corresponding strain rate. Finally, the samples would be water quenched immediately after the compression experiments to maintain the high temperature deformation microstructure. Heat treatment graph of TA15 titanium alloy compression test shown in Figure 2b.

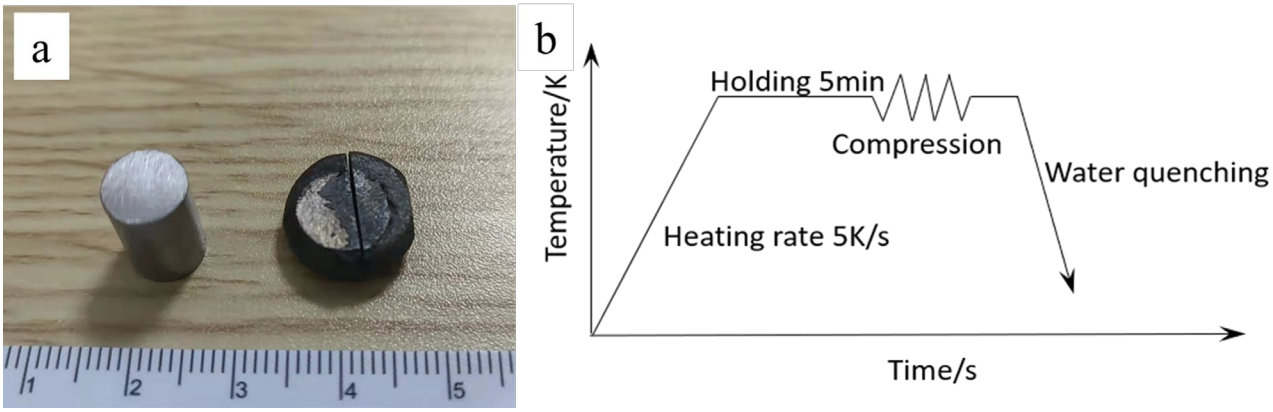

Figure 2 The appearance of specimens and the thermal compression process; (a) the appearance of specimens before and after deformation; (b) heat treatment graph in the thermal compression processing.

Results and Discussion

1. The flow stress characteristics of flow stress

The stress-strain curves of TA15 titanium alloy under different deformation conditions (1123K, 1173K, 1223K) are shown in Figure 3. As shown in the figure, when the temperature is constant, the peak stress increases as the strain rate increases. This is due to the fact that as the strain rate increases, the effect of work hardening is greater than that of α phase recrystallization. As the strain rate decreases, the flow stress reaches a stable state after the stress reaching its peak, when the strain rate decreases and the deformation time increases, the dynamic recrystallization are equivalent to the work-hardening effect[27-28].

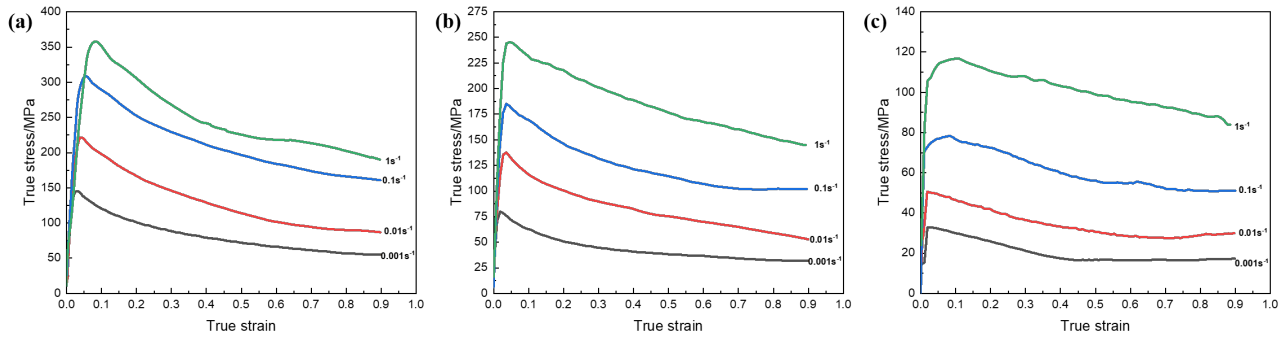

Figure 3 True-stress-strain curves at different temperature: a)1123K, b)1173K, c)1223K

2. The flow stress characteristics of flow stress

The Arrhenius constitutive model proposed by Sellars and and McTegart can accurately describe the relationship between deformation temperature, strain rate and flow stress, and is therefore widely used in the field of plastic forming[29-30]. The model can be expressed in three different ways.

$$\dot{\varepsilon}=\mathrm{A}_1\sigma^{n_1}\exp(-\frac{Q}{RT}) \tag{1}$$

$$\dot{\varepsilon}=\mathrm{A}_2\exp(\beta\sigma)\exp(-\frac{Q}{RT}) \tag{2}$$

$$\dot{\varepsilon}=\mathrm{A}[\sinh\alpha\sigma]^{n}\exp(-\frac{Q}{RT}) \tag{3}$$

where $\dot{\varepsilon}$ is the effective strain rate (s^{-1}), σ is the flow stress (MPa), T is the deformation temperature(K), Q is the thermal deformation activation energy(J/mol), R is the universal gas constants (8.314 $J/mol\cdot K$), A, A_1, A_2, α, β, n and n_1 are the material constants, and $\alpha=\frac{\beta}{n_1}$.

Eq. (2) is applicable to low stress level with ασ<0.8, and Eq. (3) is applicable to high stress level with ασ>1.2.

Taking the logarithm of both sides of Eq. (1) and (2), respectively yields:

$$\ln\dot{\varepsilon}=\ln\mathrm{A}_1+n_1\ln\sigma-Q/RT \tag{4}$$

$$\ln\dot{\varepsilon}=\ln\mathrm{A}_2+\beta\sigma-Q/RT \tag{5}$$

The material constants are solved based on the experimental data obtained from the thermal compression tests.Take the true strain of 0.2 as an example to introduce the process of solving the material constants. The test data were fitted based on Eq.(4) and Eq.(5) to obtain two sets of fitted curves.Then, the values of $n_1$and β are obtained by solving the average value of the slope of the fitted

lines, which were 5.13855 and 0.050907, respectively.And the value of α is 0.009906815 based on $\alpha = \frac{\beta}{n_1}$. Also, the value of ασ is 0.255398 to 3.02157872 and the present constitutive equation is reasonable for all strain conditions.

Taking the logarithm of both sides of Eq. (3) gives:

$$\ln[\sinh \alpha\sigma] = -\frac{1}{n}\ln A + \frac{1}{n}\ln \dot{\varepsilon} + Q/nRT \tag{6}$$

And eq. (6) can be rewritten as:

$$Q = Rn[\left\{\frac{\partial \ln[\sinh(\alpha\sigma)]}{\partial 1000/T}\right\} \tag{7}$$

It has been shown by C. Zener and H. Hollomon that the relationship between strain rate and temperature for high temperature plastic deformation of materials can be expressed in terms of the Z-parameter as follows[31-32]:

$$Z = \dot{\varepsilon}\exp(\frac{Q}{RT}) \tag{8}$$

Substituting Eq. (8) in Eq. (1) and taking the logarithm of both sides of Eq. (1) give:

$$\ln Z = \ln A + n[\ln(\sinh \alpha\sigma)] \tag{9}$$

Based on Eq.(9), it is easily found that the relationship between $\ln[\sinh(\alpha\sigma)]$ and lnZ is linear, and when the value of $\ln[\sinh(\alpha\sigma)]$ is zero, the value of lnA can be obtained. The value of A, α, n and Q are shown in Table 2.

Table 2 Constitutive model parameters of TA15 titanium alloy

A	α	n	Q
$8.25903*10^{30}$	0.009906815	3.93677	746267.9575

3. Strain-compensated Arrhenius-type constitutive model

However, when the strain is different, the model parameters of TA15 titanium alloy will change. Therefore, multiple strains of the deformation were chosen to modifyt the Arrhenius constitutive model. And the strain was selected in the range of 0.05 to 0.9 with an interval of 0.05.Then, 18 groups of model parameters were obtained by the process of solving. A ninth-order polynomial is used to represent the effect of strain on the material constants, as shown in Figure 4. The correlation coefficients of the polynomial fitting results show that the fitting accuracy is high because all four material constants are above 0.99.The coefficients of the polynomial are shown in the Table 3.

$$\begin{cases} \ln A = A_0 + A_1\varepsilon + A_2\varepsilon^2 + A_3\varepsilon^3 + A_4\varepsilon^4 + A_5\varepsilon^5 + A_6\varepsilon^6 + A_7\varepsilon^7 + A_8\varepsilon^8 + A_9\varepsilon^9 \\ \alpha = \alpha_0 + \alpha_1\varepsilon^1 + \alpha_2\varepsilon^2 + \alpha_3\varepsilon^3\alpha_4\varepsilon^4 + \alpha_5\varepsilon^5 + \alpha_6\varepsilon^6 + \alpha_7\varepsilon^7 + \alpha_8\varepsilon^8 + \alpha_9\varepsilon^9 \\ n = n_0 + n_1\varepsilon^1 + n_2\varepsilon^2 + n_3\varepsilon^3 + n_4\varepsilon^4 + n_5\varepsilon^5 + n_6\varepsilon^6 + n_7\varepsilon^7 + n_8\varepsilon^8 + n_9\varepsilon^9 \\ Q = Q_0 + Q_1\varepsilon^1 + Q_2\varepsilon^2 + Q_3\varepsilon^3 + Q_4\varepsilon^4 + Q_5\varepsilon^5 + Q_6\varepsilon^6 + Q_7\varepsilon^7 + Q_8\varepsilon^8 + Q_9\varepsilon^9 \end{cases} \tag{10}$$

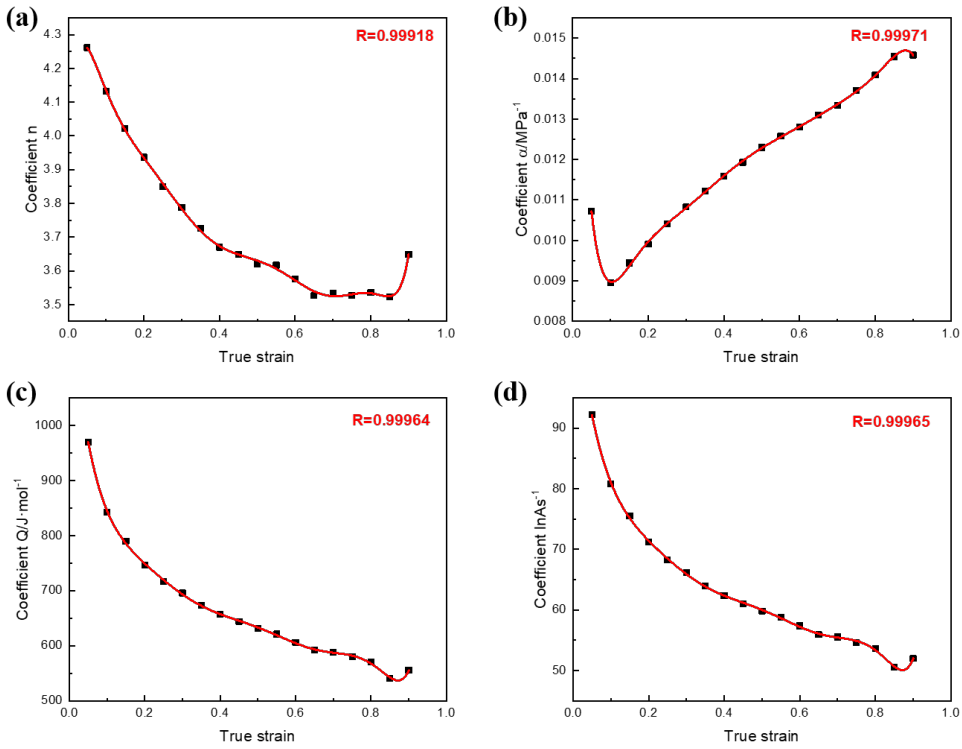

Figure 4 Variations of material constants of: a) n, b) α, c) Q and d) ln A with strain

Table 3 Coefficients of the polynomial for A, α, n, Q

	lnA		α		n		Q
A_1	112.07308	α_1	0.02038	n_1	4.12851	Q_1	1232.91434
A_2	-502.08533	α_2	-0.34552	n_2	9.7485	Q_2	-7290.291
A_3	2058.66326	α_3	4.11098	n_3	-216.97177	Q_3	47386.87474
A_4	2942.91321	α_4	-25.54035	n_4	1898.88574	Q_4	-140602.84115
A_5	-67412.25023	α_5	95.07253	n_5	-9234.04554	Q_5	-27791.82064
A_6	294948.31459	α_6	-222.38349	n_6	26834.93964	Q_6	0
A_7	-648887.42818	α_7	329.64746	n_7	-47485.7099	Q_7	0
A_8	789145.61722	α_8	-300.75517	n_8	50058.85853	Q_8	0
A_9	-505220.90521	α_9	154.16507	n_9	-28864.5825	Q_9	0
A_{10}	132993.83199	α_{10}	-33.99046	n_{10}	7002.75768	Q_{10}	0

Typically, R(Correlation coefficient) and AARE(average absolute relative error) are used to evaluate the correlation coefficient between the experimental and predicted values.Therefore, the accuracy of the established constitutive model was evaluated by calculating the R and AARE factors, and the expression is as follows:

$$R = \frac{\sum_{i}^{n}(P_i - \bar{P})(E_i - \bar{E})}{\sqrt{\sum_{i}^{n}(P_i - \bar{P})^2 \sum_{i}^{n}(E_i - \bar{E})^2}} \tag{11}$$

$$AARE = \frac{1}{n}\sum_{1}^{n}\left|\frac{P_i - E_i}{E_i}\right| \times 100 \tag{12}$$

where P_i is the predicted value, E_i is the experimental data, n is the number of data point. The comparison results of the experimental data and the predicted values are shown in the Figure 4. The correlation coefficient (R) of all deformation conditions is 0.98328.

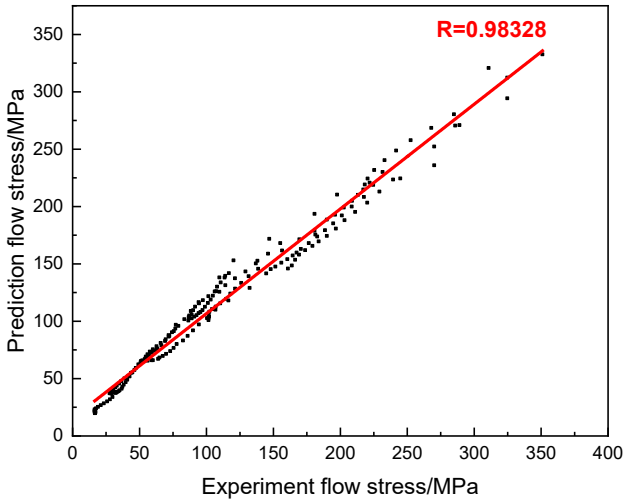

Figure 4 Correlation between the experimental and predicted flowstress data

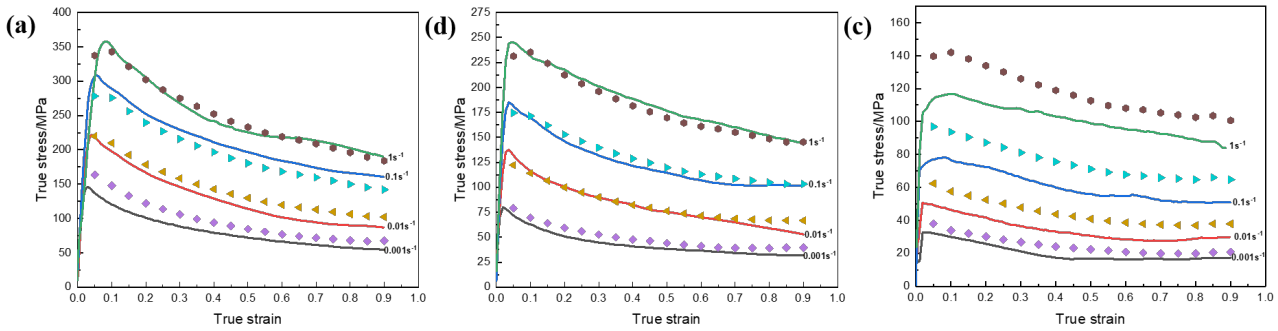

Figure 5 Comparison of the experimental and predicted flow stress at different temperatures: a)1123K, b)1173K, c)1223K

The experimental and predicted flow stress at different temperatures are shown in Figure 5. The average absolute relative error (AARE) at 1123K and 1173K is 9.8%, and the AARE at all temperature is 14.5%. which indicates that constitutive equation is well predicted for TA15 titanium alloy at 1123K and 1173K.

Conclusion

This paper investigates the flow behavior of TA15 titanium alloy through a set of hot compression test and establishes the constitutive equation. Conclusions were obtained as follows:

- TA15 titanium alloy stress is very sensitive to temperature and strain rate, the value increases with increasing strain rate and decreasing temperature. The test result curve is a typical flow curve, and the Arrhenius equation can be used to establish the constitutive model
- An Arrhenius model based on the effect of strain was established to describe the flow stress of TA15 titanium alloy. The experimental and predicted results show that the strain-compensated Arrhenius model predicts better flow behavior at 1123 K and 1173 K.
- The deviation of the predicted value of 1223K from the experimental value is influenced by the phase transformation.
- The results of the above research provide a certain basis for the hot forming of TA15 titanium alloy, and the constitutive equation can be used for FE simulation calculations.

Acknowledgement

This work acknowledges the research on the key technology of vacuum isothermal forging by the fund project of China Academy of Macinery Science and Technology Group.

References

[1] H. C. Ji, Z. S. P, W. Pei et al., Constitutive equation and hot processing map of TA15 titanium alloy[J]. Materials Research Express, 2020, 7(4), 045508.

[2] J. Li, F. G. Li, J. Cai, Constitutive Model Prediction and Flow Behavior Considering Strain Response in the Thermal Processing for the TA15 Titanium Alloy[J]. Materials, 2018, 11(10), pp1985-1985.

[3] Q. J. Sun, G. C. Wang, Microstructure and superplasticity of TA15 alloy[J]. Materials Science and Engineering A, 2014, 606, 401-408.

[4] Z. C. Sun, H. Yang, Z. Tang, Microstructural evolution model of TA15 titanium alloy based on BP neural network method and application in isothermal deformation[J]. Computational Materials Science, 2010, 50(2), 308-318.

[5] B. L. Ma, X. D. Wu, X. J. Li et al., Investigation on the hot formability of TA15 titanium alloy sheet[J]. Materials and Design, 2016, 94, 9-16.

[6] P.F. Gao, H. Yang, X.G. Fan et al., Microstructure evolution in the local loading forming of TA15 titanium alloy under non-isothermal condition[J]. Journal of Materials Processing Tech., 2012, 212(11), 2520-2528.

[7] M. Xu, W. J. Jia, Z. H. Zhang et al., Hot Compression Deformation Behavior and Processing Map of TA15 alloy[J]. Rare Metal Materials and Engineering, 2017, 46(9), 2708-2713.

[8] P. F. Gao, H. Yang, X. G. Fan et al., Microstructural features of TA15 titanium alloy under different temperature routes in isothermal local loading forming[J]. Materials Science and Engineering A, 2012, 540, 245-252.

[9] Z. Q, Li, H. T. Qu, F. L. Chen et al., Deformation Behavior and Microstructural Evolution during Hot Stamping of TA15 Sheets: Experimentation and Modelling[J]. Materials, 2019, 12(2), 223-223.

[10] Y, S, Zhang, Y, Sun, Investigation on Constitutive Equations for TA15 during Hot Working[J]. Applied Mechanics and Materials, 2012, 1867(184-185), 1492-1496.

[11] M. Li, X. Li, L. Long et al., Deformation behavior and processing map of high temperature deformation of TA15 alloy[J].Rare Metal Materials and Engineering, 2006, 35(9), 1354-1358.

[12] T. Yasmeen, Z. T. Shao, L. Zhao et al., Constitutive modeling for the simulation of the superplastic forming of TA15 titanium alloy[J]. International Journal of Mechanical Sciences, 2019, 164(C), 105178-105178.

[13] R. Zhang, D. J. Wang, L. J. Huang et al., Deformation behaviors and microstructure evolution of TiBw/TA15 composite with novel network architecture[J]. Journal of alloys and conpounds, 2017, 722, 970-980.

[14] G. Chen, Y. C. Yao, Y. Z. Jia et al., Hot Deformation Constitutive Equation and Plastic Instability of 30Cr4MoNiV Ultra-High-Strength Steel[J]. Metals, 2021, 11(5), 769-769.

[15] H. J. Cai, R. B. Song, L. Jiang et al., Plastic deformation behavior and construction of constitutive model in a wide range of strain rates of 800 MPa grade dual phase steel[J]. Mechanics of Materials, 2018, 122, pp104-117.

[16] H. Y. Wu, J. C. Yang, F. J. Zhu et al., Hot compressive flow stress modeling of homogenized AZ61 Mg alloy using strain-dependent constitutive equations[J]. Materials Science and Engineering A, 2013, 574, pp17-24.

[17] Z. M. Cai, H. C. Ji, W. C. Pei et al., Hot workability, constitutive model and processing map of 3Cr23Ni8Mn3N heat resistant steel[J].Vacuum, 2019, 165, 324-336.

[18] Z. Wang, A, Q, Wang, J, P, Xie et al., Hot Deformation Behavior and Strain-Compensated Constitutive Equation of Nano-Sized SiC Particle-Reinforced Al-Si Matrix Composites[J]. Materials, 2020, 13(8), 1812-1812.

[19] C. L. Gan, K. H. Zheng, W, J, Qi et al., Constitutive equations for high temperature flow stress prediction of 6063 Al alloy considering compensation of strain[J]. Transactions of Nonferrous Metals Society of China, 2014, 24(11), 3486-3491.

[20] L, Li, M, Q, Li, Constitutive model and optimal processing parameters of TC17 alloy with a transformed microstructure via kinetic analysis and processing maps[J]. Materials Science & Engineering A, 2017, 302-312.

[21] H. R. Wang, C. G. Wang, M. Y. Li et al., Constitutive Equations for Describing the Hot Compressed Behavior of TC4–DT Titanium Alloy[J]. Materials, 2020, 13(15).

[22] I. R. Ahmad, D.W. Shu, Compressive and constitutive analysis of AZ31B magnesium alloy over a wide range of strain rates[J]. Materials Science & Engineering A, 2014, 592

[23] X. G. Fan, H. Yang, P. F. Gao, Prediction of constitutive behavior and microstructure evolution in hot deformation of TA15 titanium alloy[J]. Materials and Design, 2013, 51, 34-42.

[24] Z. J. Yang, W. X. Yu, S. T. Lang et al., Hot Deformation Behavior and Processing Maps of a New Ti-6Al-2Nb-2Zr-0.4B Titanium Alloy[J]. Materials, 2021, 14(9),pp 2456-2456.

[25] F. H. Zhu, W. Xiong, X, F. et al., LiA new flow stress model based on Arrhenius equation to track hardening and softening behaviors of Ti6Al4V alloy[J]. Rare Metals, 2018, 37, 1035-1045.

[26] W. W. Peng, W. D. Zeng, Q, J. Wang et al., Comparative study on constitutive relationship of as-cast Ti60 titanium alloy during hot deformation based on Arrhenius-type and artificial neural network models[J]. Material &Design, 2013, 51, 95-104.

[27] J. Xiao,D. S. Li,X. Q. Li et al., Constitutive modeling and microstructure change of Ti-6Al-4V during the hot tensile deformation [J]. Journal of Alloys & Compounds, 2012, 541, 346-352.

[28] Y. Liu, J. C. Zhu, Y Wang et al., Hot compressive deformation behaviors and micro-mechanisms of TA15 alloy[J]. Rare Metels, 2007, 26(S1), 162-167.

[29] C. M. Sellars, W. J. Mctegart, On the mechanism of hot deformation[J]. Acta Metallurgica, 1966, 14(9): 1136-1138.

[30] Samantaray, D. Mandal, S. Bhaduri et al., A comparative study on Johnson Cook, modified Zerilli-Armstrong and Arrhenius-type constitutive models to predict elevated temperature flow behaviour in modified 9Cr-1Mo steel[J]. Computational Materials Science, 2009, 47, 568–576.

[31] C. Zener, J. H. Hollomon, Effect of Strain Rate Upon Plastic Flow of Steel[J]. Journal of Applied Physics, 1944, 15(1):22-32.

[32] H. Yang, Z. H. Li, Z. L. Zhang et al., Investigation on Zener-Hollomon parameter in the warm-hot deformation behavior of 20CrMnTi [J]. Journal of Zhejiang University Science A. ence, 2006, 7(8), 1433-1460.